Thermodynamic and Raman Spectroscopic Studies on Pressure-Induced Structural Transition of SF_6 Hydrate

Keisuke Sugahara, Masayoshi Yoshida, Takeshi Sugahara, and Kazunari Ohgaki*

Division of Chemical Engineering, Graduate School of Engineering Science, Osaka University, Toyonaka, Osaka 560-8531, Japan

The SF_6 hydrate system has been investigated by use of a laser Raman spectroscopic analysis in a temperature range from 274 K to 313 K and pressure up to 155 MPa. Two quadruple points have been determined at (286.6 ± 0.2) K, (1.79 ± 0.01) MPa (SF_6 hydrate + water + liquid SF_6 + gas) and at (300.3 ± 0.2) K, (131 ± 1) MPa (SF_6 hydrate + water + liquid SF_6 + solid SF_6), respectively. The structure-II SF_6 hydrate changes to the structure-I type hydrate around 33 MPa, which is a so-called "pressure-induced structural transition" of SF_6 hydrate crystal.

Introduction

Gas hydrates of crystalline substances are composed of small and large water cages capable of entrapping guest molecules, which also called clathrate hydrate. The most typical lattice structures are structure-I (space group, *Pm*3*n*),[1] structure-II (*Fd*3*m*)[1] cubic structures with unit cell formulas 2S6M·46H_2O and 16S8L·136H_2O, respectively, where small cage S is the S-cage of pentagonal dodecahedron (5^{12}) and large M and L cages are the M-cage of tetrakaidecahedron ($5^{12}6^2$) and L-cage (hexakaidecahedron, $5^{12}6^4$), respectively.

The guest species that generate the structure-II hydrate are two types. They are the small guest species less than 0.41 nm (for example,[2] Ar, Kr, N_2, and O_2) and large guest species (0.58 to 0.67) nm (such as propane,[3] THF,[4] etc.). It has been said that the smaller one occupies both cages. But that the large one only occupies the L-cage because of its volume, whereas the S-cage is vacant. We have reported about Kr[5] and N_2[6] hydrate systems in the pressure region up to 500 MPa and revealed that Kr hydrate changes to new structure crystal at high-pressure region.

SF_6 hydrate belongs to structure-II hydrate in the low-pressure region as well as propane hydrate system. The thermodynamic stability boundary for SF_6 hydrate system has been reported by several investigators.[7−9] But the thermodynamic stabilities of SF_6 hydrate at high pressure (above 100 MPa) are reported only by Dyadin et al.[7] In the present study, the five three-phase coexisting curves (SF_6 hydrate (H) + water (L_1) + gas (G)), (SF_6 hydrate (H) + water (L_1) + liquid SF_6 (L_2)), (SF_6 hydrate (H) + liquid SF_6 (L_2) + gas(G)), (water (L_1) + liquid SF_6 (L_2) + gas(G)), and (water (L_1) + liquid SF_6 (L_2) + solid SF_6 (S_2)) for the SF_6 hydrate system in a temperature range of 274 K to 313 K and pressure up to 155 MPa have been measured. The intramolecular symmetric S−F stretching vibration of SF_6 in each phase and the intermolecular O−O vibration between the water molecules are measured using laser Raman spectroscopy under the three-phase coexisting (H + L_1 + L_2) conditions. In addition, their pressure dependences are also analyzed in a pressure range up to approximately 155 MPa.

* To whom correspondence should be addressed. Phone: +81-6-6850-6290. Fax: +81-6-6850-6290. E-mail: ohgaki@cheng.es.osaka-u.ac.jp.

Experimental Section

Materials. Research grade SF_6 of mole fraction purity 99.999 % was obtained from Neriki Gas Co., Ltd. The distilled water was purchased from Yashima Pure Chemicals Co., Ltd. Both were used without further purification.

Experimental Apparatus. According to the measurement pressure region, three types of high-pressure cells (type A, type B, and, type C) were used in the present study.

1. Type A (Maximum Pressure Is 5 MPa). The high-pressure cell made of tempered glass by Taiatu Techno was essentially the same as our previous one,[10] whose inner volume and maximum working pressure were about 5 cm^3 and 5 MPa, respectively. In the inside of the cell, a magnetic stirrer bar was controlled to agitate by a permanent magnet outside. The system temperature was controlled by the thermostated water circulating from a thermocontraller (Taitec CL80 and Taitec PU-9) to water bath.

2. Type B (Maximum Pressure Is 75 MPa) and Type C (Maximum Pressure Is 400 MPa). The experimental apparatuses were essentially the same as our previous ones.[11,12] It consisted of a high-pressure cell having a couple of sapphire windows (inner volume, 1 cm^3 and 0.2 cm^3; maximum working pressure was 75 MPa and 400 MPa, respectively; Both were made of stainless steel (SUS630), a mixing ball, a high-pressure pump for supplying and/or pressurizing the samples, an intensifier, pressure gauges, a temperature control system, a charge-coupled device (CCD) camera, and a laser Raman microprobe spectrometer (Jobin Yvon Ramanor T64000). The system temperature was controlled by the thermostated water circulating from a thermocontraller through the jacket in the wall.

Procedure 1. Measurements of Three-Phase Coexisting Curves. A known amount of SF_6 was introduced into the evacuated and cooled cell. A mixing magnet or a mixing ball in the cell was vibrated from the outside for agitation. The contents were pressurized up to the desired pressure by a successive supply of water. After the formation of the SF_6 hydrate, to establish the three-phase (ex. SF_6 hydrate + water + fluid SF_6) equilibrium, the system temperature was gradually increased and the contents were agitated intermittently. The phase behavior of the system was observed by the CCD camera through the sapphire window. The equilibrium temperature was measured within a reproducibility of 0.02 K using a thermistor

10.1021/je050447t CCC: $33.50
Published on Web 12/15/2005

Table 1. Three-Phase Coexisting Curves for the SF_6 Hydrate System

p/MPa	*T*/K	*p*/MPa	*T*/K
$H + L_1 + L_2$		$H + L_2 + G$	
286.68	2.73	278.34	1.44
286.75	3.67	280.77	1.54
286.77	6.22	283.16	1.63
286.86	7.94	285.69	1.74
286.93	9.80	286.32	1.77
287.01	12.92		
287.08	14.48	$L_1 + L_2 + G$	
287.28	20.06	286.85	1.79
287.45	24.47	287.26	1.81
287.70	29.18	289.23	1.91
287.82	30.18	291.20	2.00
288.32	34.47	293.19	2.10
289.22	39.64	295.14	2.20
289.52	40.78		
291.23	50.18	$L_1 + L_2 + S_2$	
293.27	60.69	313.25	155
294.38	70.12	308.12	145
295.45	80	303.51	137
296.64	88	301.89	134
297.80	97	300.41	131
298.92	113		
299.85	125		
$H + L_1 + G$		Q_2	
274.28	0.10	286.6	1.79
275.78	0.14		
278.45	0.25	Q_3	
279.54	0.31	300.3	131
280.90	0.43		
282.04	0.56	Structural-Transition Point	
283.17	0.73	288	33
284.22	0.94		
285.24	1.22		
285.81	1.42		
286.05	1.53		
286.18	1.59		

probe (Takara D-641) calibrated by a Pt resistance thermometer (25 Ω) into the water bath or a hole in the cell wall. For pressure measurement, two different pressure gauges were used according to the working pressure. Up to 75 MPa, a pressure gauge (Valcom VPRT) calibrated by a Ruska quartz Bourdon tube gauge was used with an estimated maximum uncertainty of 0.02 MPa. Over 75 MPa, a pressure transducer (NMB STD-5000K) and digital peak holder (NMB CSD-819) were used with an estimated maximum uncertainty of 2 MPa.

Procedure 2. Raman Spectroscopic Analysis. The single crystal of the SF_6 hydrate prepared in the high-pressure optical cell (type C) was analyzed using a laser Raman microprobe spectrometer with a multichannel CCD detector. The light source for excitation was argon ion laser whose wavelength, power level, and spot diameter were 514.5 nm, 100 mW, and 2 μm, respectively. The laser beam from the object lens was irradiated to the SF_6 hydrate through a sapphire window, and the backscatter of the opposite direction was taken in with the same lens. The CCD detector was kept at (140 ± 5) K by liquid nitrogen for heat−noise reduction. The integration time was varied from (60 to 300) s, depending on the intensity of light scattering. The slit width was 300 μm. The spectral resolution was about 1 cm^{-1}. The SF_6 molecule has three Raman active vibration modes. In the present study, we noticed the symmetric S−F stretching vibration mode (ν_1: detected at 774 cm^{-1} at atmospheric pressure[13] because it is sharp and intensive).

Results and Discussion

The three-phase coexisting curves for the SF_6 hydrate system are listed in Table 1 and plotted on the plane of logarithmic pressure versus temperature in Figure 1 accompanied by the data of Dyadin et al.[7] The ($H + L_2 + G$) and ($L_1 + L_2 + G$) curves lie above the saturated vapor-pressure curve of SF_6. The ($H + L_2 + G$) curve intersects the ($H + L_1 + G$) curve at lower quadruple point Q_2 ($H + L_1 + L_2 + G$) of (286.6 ± 0.2) K and (1.79 ± 0.01) MPa. The ($H + L_1 + L_2$) curve originates from Q_2. From the discontinuity of d*p*/d*T* on the stability boundary ($H + L_1 + L_2$) around 33 MPa, the structural-phase transition point has also been determined at (288.0 ± 0.3) K and (33 ± 1) MPa. According to Dyadin et al.,[7] the structural-phase transition of SF_6 hydrate occurs at 288.2 K and 33 MPa. Our datum agrees well with that of Dyadin et al. From the cross-point of ($H + L_1 + L_2$) and ($L_1 + L_2 + S_2$) curves, we have determined the higher quadruple point Q_3 ($H + L_1 + L_2 + S_2$) of (303.3 ± 0.2) K and (131 ± 1) MPa. Dyadin et al.[7] have claimed the second structural-phase transition point at 301.2 K and 132 MPa. It is very near to our higher quadruple point (Q_3). Unfortunately, our apparatus was not suitable to measure the three-phase coexisting ($H + L_1 + S_2$) and ($H + L_2 + S_2$) curves. Therefore, the second structural-phase transition point cannot be determined.

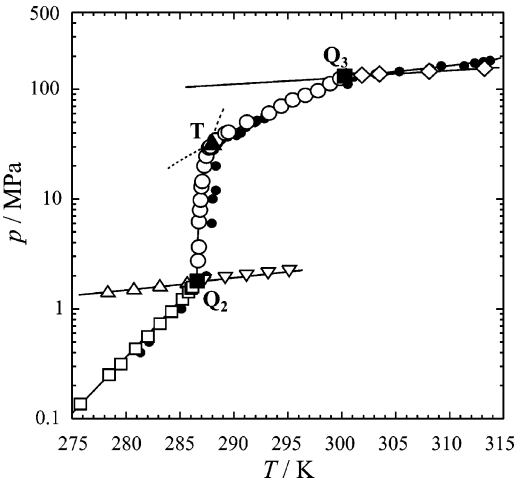

Figure 1. Three-phase coexisting curves for the SF_6 hydrate system: □, $H + L_1 + G$; △, $H + L_2 + G$; ○, $H + L_1 + L_2$; ▽, $L_1 + L_2 + G$; ◇, $L_1 + L_2 + S_2$; ■, quadruple point; ▲, phase-transition point; ●, ref 7.

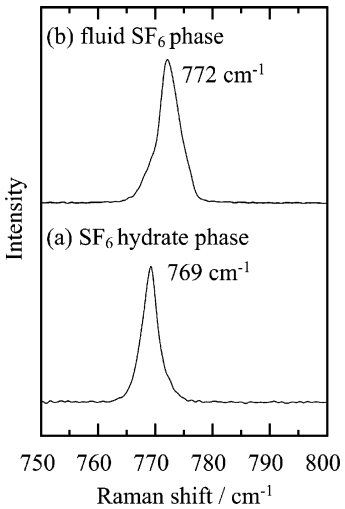

Figure 2. Raman spectra of the symmetric S−F stretching vibration mode of SF_6 molecules at 20MPa: (a) SF_6 hydrate phase; (b) fluid SF_6 phase.

Typical Raman spectra for the SF_6 hydrate system at 20 MPa are shown in Figure 2. The Raman peak of SF_6 molecules dissolved in the liquid water phase cannot be analyzed because it is very weak. On the other hand, a single Raman peak is

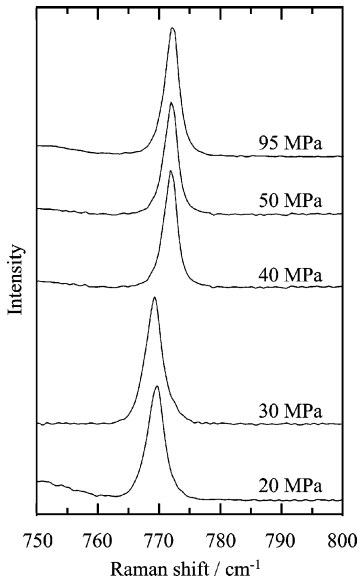

Figure 3. Raman spectra of the symmetric S−F stretching vibration in the SF_6 hydrate crystal on thermodynamic stability boundary.

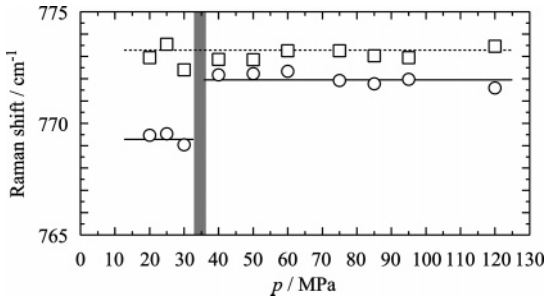

Figure 4. Pressure effect on the symmetric S−F stretching vibration in the SF_6 hydrate system: ○, hydrate phase; □, fluid phase.

detected around 769 cm^{-1} and 773 cm^{-1} for the symmetric S−F stretching vibration in the SF_6 hydrate (Figure 2a) and fluid SF_6 (Figure 2b) phases, respectively. This result reveals that the SF_6 molecule can occupy only the L-cage of the structure-II unit lattice. Above 40 MPa, the single Raman peak in the SF_6 hydrate phase is detected around 772 cm^{-1} as shown in Figure 3, and it is constant in the whole pressure region above 40 MPa.

The pressure dependence of the Raman shift for the symmetric S−F stretching vibration is summarized in Figure 4. The Raman shift in the SF_6 fluid phase is detected at 773 cm^{-1} in the whole pressure range of the present study. The Raman shift in the SF_6 hydrate phase is detected at 769 cm^{-1} in the pressure range up to 30 MPa. While the Raman shift exhibits a 3 cm^{-1} blue shift above 33 MPa; that is, SF_6 hydrate changes the crystal latttice from the structure-II to the structure-I type near 33 MPa. According to the neutron diffraction experiment of Dyadin et al.,[7] the structure-II SF_6 hydrate changes to the structure-I hydrate at 33 MPa. Our results agree well with that of Dyadin et al.[7]

We have reported that the Raman shift of the intermolecular O−O stretching vibration mode of water molecules was usually detected around 205 cm^{-1} for structure-I hydrate crystals in the low-pressure region.[12,14−18] The Raman shift of the intermolecular O−O vibration mode in the SF_6 hydrate crystal is detected at 210 cm^{-1} as shown in Figure 5 and agrees well with that of the structure-II THF hydrate crystal in the similar pressure region.[19] The Raman shift of the O−O vibration for the Kr[5] and N_2[6] hydrates, both belonging to the structure-II

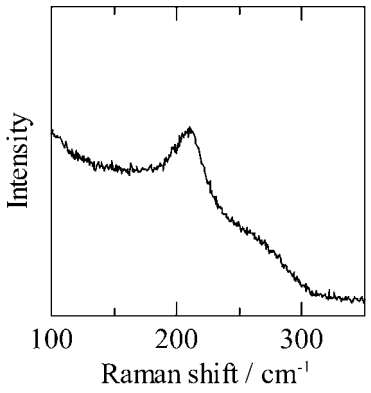

Figure 5. Raman spectrum of the intermolecular O−O vibration mode in the SF_6 hydrate crystal at 30 MPa.

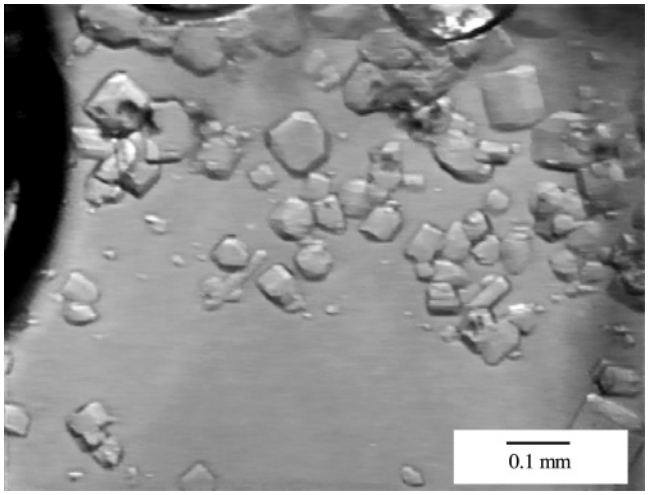

Figure 6. Single crystals of SF_6 hydrate at 293 K and 60 MPa.

hydrate, is obtained around 209 cm^{-1} from the extrapolation of their pressure dependence. These facts reveal that the Raman shift of the O−O vibration of structure-II hydrates exhibits 5 cm^{-1} higher frequencies than that of structure-I regardless of S-cage occupancies.

Above 40 MPa, the SF_6 hydrate changes to the structure-I. Therefore, it was supposed that the Raman peak of O−O vibration was detected around 205 cm^{-1}. However, the O−O vibration peak is vanished in a pressure region from 40 MPa to 120 MPa, even if the hydrate crystal seems to be apparently single crystal as shown in Figure 6. It is certain that the pressure where the Raman peak disappears coincides with the structural transition point. At the pressure, the SF_6 molecule is removed into the M-cage of structure-I from the L-cage of structure-II by pressurization. We speculate that the M-cage would be modified and distorted by taking the SF_6 molecule in forcibly. However, the peak disappearance is not interpreted sufficiently at the present time.

Conclusions

Three-phase coexisting curves of SF_6 hydrate system were obtained up to 155 MPa by use of high-pressure optical cell. Two quadruple points (four phases coexisting points; Q_2 and Q_3) were determined at (286.6 ± 0.2) K, (1.79 ± 0.01) MPa (Q_2; SF_6 hydrate + water + liquid SF_6 + gas), and at (300.3 ± 0.2) K, (131 ± 1) MPa (Q_3; SF_6 hydrate + water + liquid SF_6 + solid SF_6), respectively. From the discontinuity of dp/dT on the stability boundary at 33 MPa, the structural phase transition point was also determined at (288 ± 0.2) K and (33 ± 1) MPa.

The pressure dependence of the Raman shift for the symmetric S−F stretching vibrational mode also supports that the pressure-induced structural transition occurs in the pressure region near 33 MPa. These facts indicate that the structure-II SF_6 hydrate changes to a different structure hydrate (probably structure-I) at the pressure.

Acknowledgment

K.S. expresses his special thanks to the Center of Excellence (21COE) program "Creation of Integrated Eco-Chemistry of Osaka University". We are grateful to the Division of Chemical Engineering, Graduate School of Engineering Science, Osaka University, for the scientific support by "Gas-Hydrate Analyzing System (GHAS)".

Literature Cited

(1) Stackelberg, M. V.; Müler, H. R. Feste gashydrate II. *Z. Elektrochem.* **1954**, *58*, 25−39.
(2) Davidson, D. W.; Handa, Y. P.; Ratcliffe, C. I.; Tse, J. S.; Powell, B. W. The ability of small molecules to form clathrate hydrates of structure-II. *Nature* **1984**, *311*, 142−143.
(3) Sloan, E. D., Jr. Fundamental principles and applications of natural gas hydrates. *Nature* **2003**, *426*, 353−359.
(4) Manakov, A. Y.; Goryainov, S. V.; Kurnosov, A. V.; Likhacheva, A. Y.; Dyadin, Y. A.; Larionov, E. G. Clathrate nature of the high-pressure tetrahydrofuran hydrate phase and some new data on the phase diagram of the tetrahydrofuran−water system at pressures up to 3 GPa. *J. Phys. Chem. B* **2003**, *107*, 7861−7866.
(5) Sugahara, K.; Sugahara, T.; Ohgaki, K. Thermodynamic and Raman spectroscopy studies of Xe and Kr hydrates. *J. Chem. Eng. Data* **2005**, *50*, 274−277.
(6) Sugahara, K.; Tanaka, Y.; Sugahara, T.; Ohgaki, K. Thermodynamic stability and structure of nitrogen hydrate crystal. *J. Supramol. Chem.* **2002**, *2*, 365−368.
(7) Dyadin, Y. A.; Larionov, E. G.; Manacov, A. Y.; Kurnosov, A. V.; Zhurko, F. V.; Aladko, E. Y.; Aladko, A. I.; Tolochko, B. P.; Sheromov, M. A. Clathrate hydrate of sulfer hexafloride at high pressures. *J. Inclusion Phenom. Macrocyclic Chem.* **2002**, *42*, 213-218.
(8) Miller, S. L.; Eger, E. I.; Lundgreen, C. Anasthetic potency of CF_4 and SF_6 in dogs. *Nature* **1969** *221*, 468−469.
(9) Sortland, L. D.; Robinson, D. B. The hydrates of methane and sulphur hexafluoride. *Can. J. Chem. Eng.* **1964**, *February*, 38−41.
(10) Shimada, N.; Sugahara, K.; Sugahara, T.; Ohgaki, K. Phase transition from structure-H to structure-I in the methylcyclohexane + xenon hydrate system. *Fluid Phase Equilib.* **2003**, *205*, 17−23.
(11) Ohgaki, K.; Hamanaka, T. Phase-behavior of CO_2 hydrate−liquid CO_2−H_2O system at high pressure. *Kagaku Kougaku Ronbunshu* **1995**, *21*, 800−803.
(12) Nakano, S.; Moritoki, M. Ohgaki, K. High-pressure phase equilibrium and Raman microprobe spectroscopic studies on the CO_2 hydrate system. *J. Chem. Eng. Data* **1998**, *43*, 807−810.
(13) Rubin, B.; McCubbin, T. K., Jr; Polp, S. R. Vibrational Raman spectrum of SF_6. *J. Mol. Spectrosc.* **1978**, *69*, 254−259.
(14) Nakano, S.; Moritoki, M. Ohgaki, K. High-pressure phase equilibrium and Raman microprobe spectroscopic studies on the methane hydrate system. *J. Chem. Eng. Data* **1999**, *44*, 254−257.
(15) Morita, K.; Nakano, S.; Ohgaki, K. Structure and stability of ethane hydrate crystal. *Fluid Phase Equilib.* **2000**, *169*, 167−175.
(16) Sugahara, T.; Morita, K.; Ohgaki, K. Stability boundaries and small hydrate-cage occupancy of ethylene hydrate system. *Chem. Eng. Sci.* **2000**, *55*, 6015−6020.
(17) Suzuki, M.; Tanaka, Y.; Sugahara, T.; Ohgaki, K. Pressure dependence of small-cage occupancy in the cyclopropane hydrate system. *Chem. Eng. Sci.* **2001**, *56*, 2063−2067.
(18) Sugahara, K.; Yoshida, M.; Sugahara, T.; Ohgaki, K. High-pressure phase behavior and cage occupancy for the CF_4 hydrate system. *J. Chem. Eng. Data* **2004**, *49*, 326−329.
(19) Takasu, Y.; Iwai, K.; Nishio, I. Low-frequency Raman profiles of type-II clathrate hydrate of THF and its application for phase identification. *J. Phys. Soc. Jpn.* **2003**, *72*, 1287−1291.

Received for review October 24, 2005. Accepted November 7, 2005.

JE050447T